

Piecewise 1D laterally constrained inversion of resistivity data

Esben Auken,* Anders V. Christiansen, Bo H. Jacobsen, Nikolaj Foged and Kurt I. Sørensen

The HydroGeophysics Group, University of Aarhus, Finlandsgade 8, 8200 Aarhus, Denmark

Received January 2003, revision accepted October 2004

ABSTRACT

In a sedimentary environment, layered models are often capable of representing the actual geology more accurately than smooth minimum structure models. Furthermore, interval thicknesses and resistivities are often the parameters to which non-geophysicist experts can relate and base decisions on when using them in waste site remediation, groundwater modelling and physical planning.

We present a laterally constrained inversion scheme for continuous resistivity data based on a layered earth model (1D). All 1D data sets and models are inverted as one system, producing layered sections with lateral smooth transitions. The models are regularized through laterally equal constraints that tie interface depths and resistivities of adjacent layers. Prior information, e.g. originating from electric logs, migrates through the lateral constraints to the adjacent models, making resolution of equivalences possible to some extent. Information from areas with well-resolved parameters will migrate through the constraints in a similar way to help resolve the poorly constrained parameters. The estimated model is complemented by a full sensitivity analysis of the model parameters, supporting quantitative evaluation of the inversion result.

Examples from synthetic 2D models show that the model recognition of a sublayered 2D wedge model is improved using the laterally constrained inversion approach when compared with a section of combined 1D models and when compared with a 2D minimum structure inversion. Case histories with data from two different continuous DC systems support the conclusions drawn from the synthetic example.

INTRODUCTION

Electrical methods have been used successfully for a long time in environmental and hydrogeophysical studies (Fitterman 1987; Dodds and Ivic 1990; Sandberg and Hall 1990; Taylor, Widmer and Chesley 1992; Robineau *et al.* 1997; Albouy *et al.* 2001). Nowadays, standard methods allow a more detailed mapping by continuously gathering profile orientated data using either multiple electrode systems, such as the continuous vertical electrical sounding (CVES) system (Dahlin 1996; Bernstone and Dahlin 1999) or systems like the pulled ar-

ray continuous electrical sounding (PACES) system (Sørensen 1996) and others (Panissod, Lajarthe and Tabbagh 1997). Programs for inverting single sounding data with 1D models have been available for a number of years (e.g. Inman, Riju and Ward 1975; Johansen 1977). Both the CVES and the PACES methods result in dense profile-orientated data coverage with large sensitivity overlaps between individual soundings. This, of course, is very suitable for 2D interpretations but unfortunately 2D inversion is still a relatively slow process, considering the amount of data collected. Furthermore, the most widely used routines produce smooth earth models (Oldenburg and Li 1994; Loke and Barker 1996) in which formation boundaries are hard to recognize. This is not as severe when using a robust inversion scheme (the L_1 -norm) as when

*E-mail: esben.auken@geo.au.dk

using standard least-squares schemes (Loke *et al.* 2003), but layer boundaries are still smeared out.

Several authors have combined the use of 2D and 1D calculations to achieve a faster code than that obtained with 2D calculations alone (e.g. Oldenburg and Ellis 1991; Smith and Booker 1991; Christiansen and Auken 2003).

Gyulai and Ormos (1999) presented a 1.5D procedure for interpretation of vertical electrical sounding (VES) data using 1D calculations only. They connected soundings on a profile by describing the lateral variations using sine and cosine power functions expanded into series. This way of connecting soundings creates a laterally smooth layered model. Santos (2004) combined a 2D roughness matrix with 1D calculations to produce laterally homogeneous models using only the 1D information.

We present a piecewise 1D laterally constrained inversion (LCI) scheme capable of performing inversion of very large data sets. The primary parameters of the earth model are resistivities and thicknesses. The models are connected laterally by requiring approximate identity between neighbouring parameters, typically resistivity and depth, within a specified variance. The lateral constraints can be considered as *a priori* information on the geological variability within the area where the measurements are taken. A series of soundings is inverted as one system providing layered and laterally smooth model sections. Prior information, originating from, for example, electrical logs, can be added at any point of the profile and the information migrates through the lateral constraints to the adjacent nodes. The inversion result is supported by a full sensitivity analysis of the model parameters. It is essential in most geophysical investigations to ascertain the quality of the inversion result. The resulting model section is laterally smooth with sharp layer interfaces as depicted in Fig. 1.

The development of the piecewise 1D LCI formalism is closely linked to the development of instrumentation and field methodologies to ensure that the interpretation tools used can handle the large data volumes and extract the maximum

amount of information. The piecewise 1D formalism was developed based on the following considerations:

- In a sedimentary environment the subsurface is often sub-layered with relatively slow lateral variations.
- Inversion of single-site DC data suffers greatly from equivalences. Adding information on the lateral continuity of layers should improve the resolution of layers affected by equivalences.
- The inversion scheme must be fast and capable of handling large data sets, and it must be robust to different starting models, i.e. it must converge safely when initiated from a homogeneous half-space.
- There must be an option to include geophysical prior information at any given point.
- The output model must be accompanied by a sensitivity analysis of the model parameters.

This paper demonstrates that the LCI algorithm provides a practical interpretation tool that meets these design criteria. However, it is not our aim to design an inversion scheme capable of resolving 2D structures with a 1D formulation. We focus on improved resolution for models with slow lateral variations that apply well to the 1D formulation with lateral constraints.

DATA ACQUISITION SYSTEMS

The examples given in this paper are based on data from the CVES and the PACES systems and we therefore give a brief overview of these systems.

The CVES system consists of a number of steel electrodes (typically about 60, depending on the system type) manually forced into the ground at a regular electrode spacing, typically from 5 to 12 m (Van Overmeeren and Ritsema 1988; Dahlin 1996, 2001).

The PACES system consists of a small tractor, equipped with processing electronics, pulling electrodes mounted on a tail (Sørensen 1996; Sørensen *et al.* 2005). The electrodes are

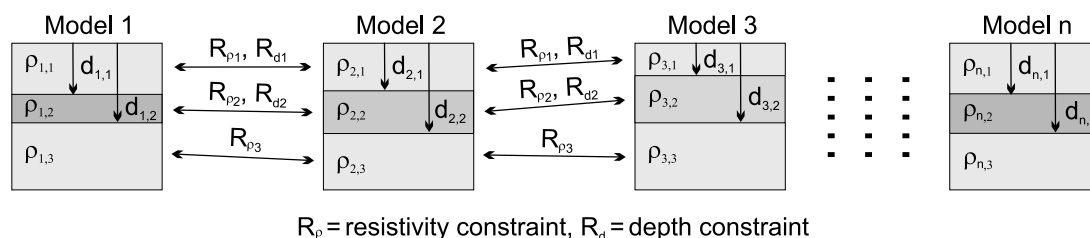


Figure 1 Laterally constrained inversion (LCI) model set-up.

cylindrical steel tubes with a weight of 10–20 kg. Two electrodes are maintained as current electrodes with a maximum current of 30 mA. The remaining electrodes serve as potential electrodes in eight different configurations. The electrode configurations are both symmetric Wenner configurations as well as highly asymmetric configurations for an optimal data acquisition to resolve a wide variety of structures.

INVERSION METHODOLOGY

Model set-up

The model is a section of laterally constrained 1D models along a profile as sketched in Fig. 1. The lateral distance between the models is controlled by the sampling density of the data and may be non-equidistant. The layer parameters are resistivities and thicknesses. The bottom layer extends to infinite depth. The collection of DC data with multielectrode systems is usually arranged so that the data set is suited for inversion using 2D smooth inversion algorithms. However, in this application the data sets are divided into soundings where all data with a lateral focus point in a specific section combine into a data set (a sounding) referring to one 1D model. The lateral focus points of the asymmetric configurations of the PACES system have been found by numerical integration of the 2D sensitivity distributions. PACES data are usually divided into soundings with a spacing of 5 or 10 m.

Inversion set-up

A detailed description of the inversion algorithm and the practical implementation of the constraints has been given by Auken and Christiansen (2004). A short summary is given here. The dependence of apparent resistivity on subsurface parameters is in general described as a non-linear differentiable forward mapping. We follow the established practice of linearized approximation with the first term of the Taylor expansion,

$$\mathbf{d}_{\text{obs}} + \mathbf{e}_{\text{obs}} \cong \mathbf{G}(\mathbf{m}_{\text{true}} - \mathbf{m}_{\text{ref}}) + \mathbf{g}(\mathbf{m}_{\text{ref}}), \quad (1)$$

where \mathbf{d}_{obs} denotes the observed data, \mathbf{e}_{obs} denotes the error on the observed data and \mathbf{g} is the non-linear mapping of the model to the data space. The true model \mathbf{m}_{true} has to be sufficiently close to some arbitrary reference model, \mathbf{m}_{ref} , for the linear approximation to be valid. The covariance matrix for the observation errors is \mathbf{C}_{obs} , which we assume to be a diagonal matrix. In short, we write

$$\mathbf{G}\delta\mathbf{m}_{\text{true}} = \delta\mathbf{d}_{\text{obs}} + \mathbf{e}_{\text{obs}}. \quad (2)$$

The Jacobian matrix \mathbf{G} contains the partial derivatives of the mapping, i.e.

$$G_{st} = \frac{\partial d_s}{\partial m_t} = \frac{\partial \log(d_s)}{\partial \log(m_t)} = \frac{m_t}{d_s} \frac{\partial d_s}{\partial m_t}, \quad (3)$$

which also ensures positivity of the data and the model parameters (e.g. Johansen 1977; Ward and Hohmann 1988).

The constraints are connected to the true model as

$$\mathbf{R}\delta\mathbf{m}_{\text{true}} = \delta\mathbf{r} + \mathbf{e}_r, \quad (4)$$

where \mathbf{e}_r is the error on the constraints with 0 as expected value, and $\delta\mathbf{r} = -\mathbf{R}_p\mathbf{m}_{\text{ref}}$ provides the identity between the parameters tied by constraints in the roughening matrix \mathbf{R} , containing 1s and -1 s for the constrained parameters, 0 in all other places. The variance, or strength of the constraints, is described in the covariance matrix \mathbf{C}_R . In this approach we only operate with lateral constraints although vertical constraints can be used as well. The strength or variance of the constraints depends on the expected variation in the underlying geological model. Small constraints allow only for small model changes and vice versa. Hence, the constraints are ideally determined for each data set based on an evaluation of the stochastic properties of the underlying geological features. Practical experiments show that constraint values between 1.1 and 1.3 are good starting options. Roughly speaking, a constraint value of 1.1 means that model parameters are allowed to vary 10% between neighbouring models.

Combining (2) and (4), we may write the inversion problem as

$$\begin{bmatrix} \mathbf{G} \\ \mathbf{R} \end{bmatrix} \delta\mathbf{m}_{\text{true}} = \begin{bmatrix} \delta\mathbf{d}_{\text{obs}} \\ \delta\mathbf{r} \end{bmatrix} + \begin{bmatrix} \mathbf{e}_{\text{obs}} \\ \mathbf{e}_r \end{bmatrix}, \quad (5)$$

or, more compactly,

$$\mathbf{G}'\delta\mathbf{m}_{\text{true}} = \delta\mathbf{d}' + \mathbf{e}'. \quad (6)$$

If *a priori* data are present another row is added to (5). The covariance matrix for the joint observation error \mathbf{e}' becomes

$$\mathbf{C}' = \begin{bmatrix} \mathbf{C}_{\text{obs}} & 0 \\ 0 & \mathbf{C}_R \end{bmatrix}. \quad (7)$$

The model estimate (Menke 1989),

$$\delta\mathbf{m}_{\text{est}} = (\mathbf{G}'^T \mathbf{C}'^{-1} \mathbf{G}')^{-1} \mathbf{G}'^T \mathbf{C}'^{-1} \delta\mathbf{d}', \quad (8)$$

minimizes

$$Q = \left(\frac{1}{N+A} [(\delta\mathbf{d}'^T \mathbf{C}'^{-1} \delta\mathbf{d}')] \right)^{\frac{1}{2}}, \quad (9)$$

where A is the number of constraints and N is the number of data.

In other words, all data sets are inverted simultaneously, minimizing a common object function, and the number of output models is equal to the number of 1D soundings included. The lateral constraints and the data are all part of the inversion. Consequently, the output models are balanced between the constraints, the physics and the data. Model parameters that have little influence on the data will be controlled by the constraints, and vice versa. Due to the lateral constraints, information from one model will spread to the neighbouring models.

Implementation of the forward response

Forward responses are calculated as a summation of pole-pole responses over a layered earth as described by Telford *et al.* (1990). The potentials are computed using the Hankel transform filters of Johansen and Sørensen (1979) as calculated by Christensen (1990).

Analysis of model estimation uncertainty

The sensitivity analysis of model parameters from 1D laterally constrained inversion can be used to assess the resolution of the inverted model. The parameter sensitivity analysis of the final model is the linearized approximation of the covariance of the estimation error, C_{est} (e.g. Tarantola and Valette 1982), given by

$$C_{\text{est}} = (\mathbf{G}^T \mathbf{C}' \mathbf{G})^{-1}. \quad (10)$$

Standard deviations on model parameters are calculated as the square root of the diagonal elements in C_{est} . For mildly non-linear problems, this is a good approximation. Because the model parameters are represented as logarithms, the analysis gives a standard deviation factor (*STDF*) for the parameter m_s , defined by

$$STDF(m_s) = \exp\left(\sqrt{C_{\text{est},ss}}\right). \quad (11)$$

Thus, the theoretical case of perfect resolution has $STDF = 1$. A factor of $STDF = 1.1$ is approximately equivalent to an error of 10%. Roughly speaking, for well-resolved parameters $STDF < 1.2$, for moderately resolved parameters $1.2 < STDF < 1.5$, for poorly resolved parameters $1.5 < STDF < 2$, and for unresolved parameters $STDF > 2$.

Computation times

A system with 100 separate 1D models with a total of 500 model parameters and 100 PACES data sets (a total of 800

data) uses approximately 4 seconds for one iteration on a Pentium4, 2 GHz, machine. Depending on the model, between 10 and 20 iterations are normally needed to converge to a satisfactory misfit level. The matrix operations are the primary time-consuming operations of the inversion scheme. Hence, inverting smaller data sets and model sections reduces the computation time significantly.

SYNTHETIC EXAMPLE

The synthetic data (see Fig. 2) are calculated using the 2D finite-difference forward program, DCIPF2D, developed at the University of British Columbia (Dey and Morrison 1979; McGillivray 1992).

Analyses on model parameters are calculated using (10) and are presented together with the inversions. We use a colour-grading of the *STDF* in (11) of resistivity and thickness, ranging from well-determined (red) to undetermined (blue).

Data were calculated for the PACES system every 1 m, perturbed with 5% Gaussian noise, and subsequently processed in a similar way to the actual processing of field data (Sørensen *et al.* 2005). The resulting distance between soundings is 5 m.

Geophysically, this model is fairly one-dimensional and it deals with the identification of thin layers that might suffer from equivalences. Geologically, the example illustrates a typical hydrogeological model where the focus is the delineation of low-resistivity clay or moraine layers. Near-surface clayey layers are important for the protection of underlying aquifers (Sørensen *et al.* 2005). The models in Fig. 2(a,b) consist of a 4 m-thick layer at a depth of 3 m. The layer is thinner at the middle, and it vanishes in the central part of the section. The resistivities of the layer and the surroundings in Fig. 2(a) are 40 Ωm and 200 Ωm , respectively. This is reversed for the model in Fig. 2(b). A stochastic variation is superimposed on the layer resistivities to resemble an actual geological formation more closely. The question is whether it is possible to map both the layer and its absence reasonably accurately, knowing that the second layer is predisposed to equivalence (Fitterman, Meekees and Ritsema 1988).

The combined 1D inversions without constraints on parameters (Fig. 2c,d) give the overall geometry of the models, but it is clear that especially the central part of the model shows high/low resistivity equivalence. This is confirmed when watching the poorly constrained parameters in the analyses in Fig. 2(e,f). The models close to where the second layer is missing are all affected by 2D effects from the edges, showing pant-leg effects. The somewhat jagged appearance of the section is due to the 5% noise added to the data.

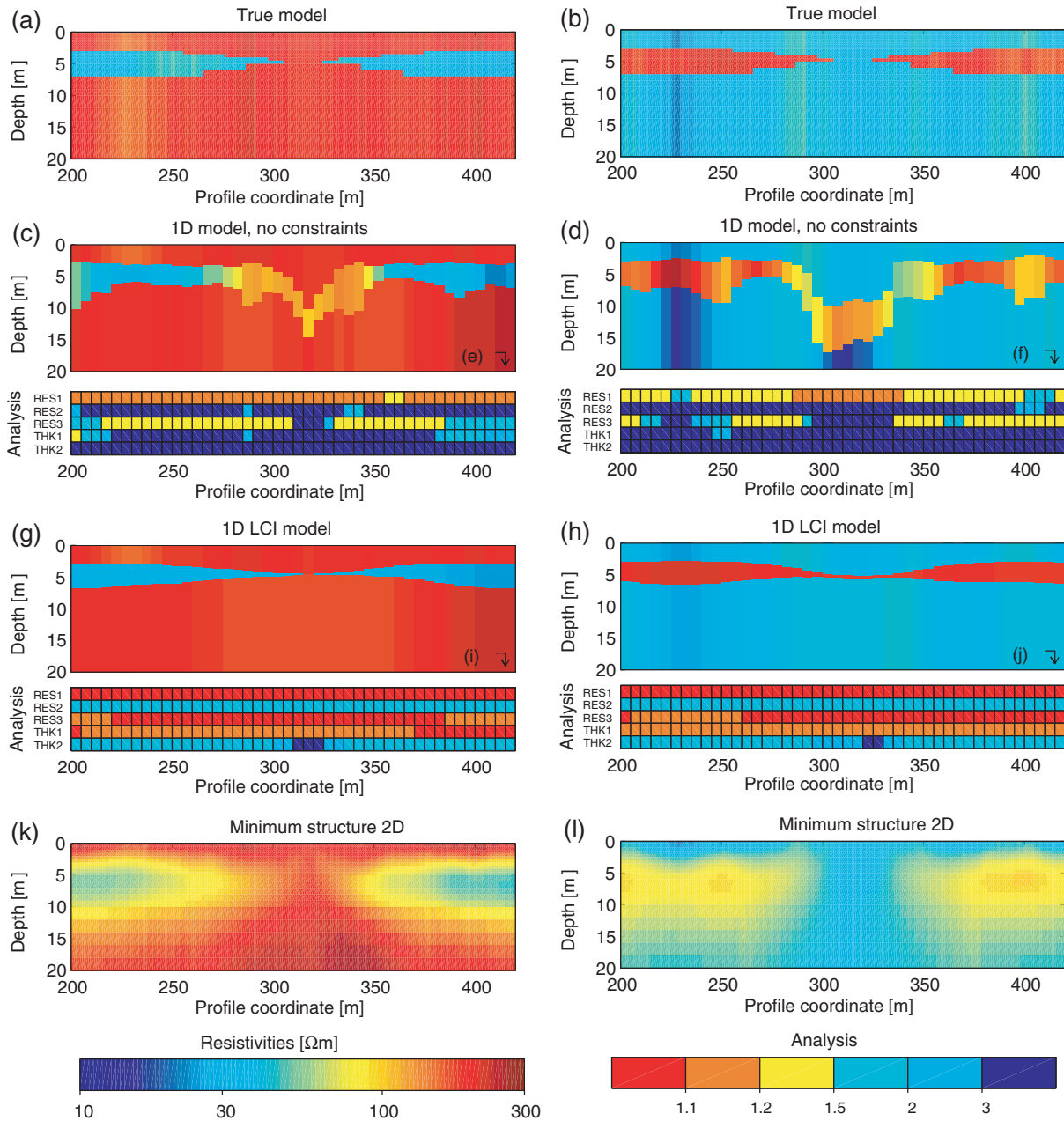


Figure 2 Synthetic examples: PAGES. (a) and (b) The true 2D model. (c) and (d) Standard combined 1D inversions with no constraints on the model parameters. (e) and (f) Analyses of the primary parameters in the model, ranging from well-resolved (red) to poorly resolved (blue). (g)–(j) Repeats of (c)–(f), but now as LCI with lateral constraints on depth and resistivity. (k) and (l) A minimum structure 2D inversion of the profiles. The sounding distance is 5 m.

The laterally constrained models in Fig. 2(g,h) minimize the effects of both 2D effects and equivalences. In this case, the values of the constraints are a factor of 1.14 on both depths to layer boundaries and on resistivities.

The analyses on the model parameters in Fig. 2(i,j) reveal an improved resolution, especially in layers 1 and 3. With the

equivalences, layer 2 is still poorly resolved, but slightly better than was the case with unconstrained models.

For comparison we have inverted the section using a standard least-squares minimum-structure 2D inversion. For this purpose we have used the DCINV2D program (Oldenburg and Li 1994). The inversion results are presented in Fig. 2(k,l).

The inversion result shows a smeared image of the true model. The original layer boundaries are hard to recognize and the hole in the layer appears much wider than it actually is.

From a large number of numerical simulations, given a layered earth with relatively smooth transitions in resistivities and layer boundaries, the laterally constrained inversion produces results that resemble the actual model well (Auken, Foged and Sørensen 2002). Resolution of individual parameters is improved compared with ordinary 1D inversion, as is resolution of potential equivalences.

FIELD EXAMPLES

There are many field examples of the PACES and the CVES systems, since both systems have been used extensively over the last decade. We present two examples, the first from a CVES survey in southern Sweden, the second from a regional (100 line km) PACES survey in Jutland, Denmark.

CVES example, southern Sweden

Figure 3 shows the interpretation of a 300 m profile from the southern part of Sweden. The resistivity survey was carried out as part of the geotechnical investigations for road construction in connection with the motorway connections to the Öresund bridge–tunnel between Denmark and Sweden. Figure 3(a) shows the data pseudosection, Fig. 3(b) is a minimum-structure 2D inversion, and Fig. 3(c) is a combined 1D model section with the accompanying analysis shown in Fig. 3(d). Figure 3(e,f) shows the laterally constrained inversion model and the parameter analysis, respectively. The constraints between resistivities and depth interfaces used in the LCI inversion form a factor of 1.14.

The data pseudosection in Fig. 3(a) shows relatively smooth transitions and there are no clear signs of characteristic 2D structures, although near-surface resistivity variations can be recognized at, for example, profile coordinate 150 m. The minimum structure 2D inversion in Fig. 3(b) reveals a number

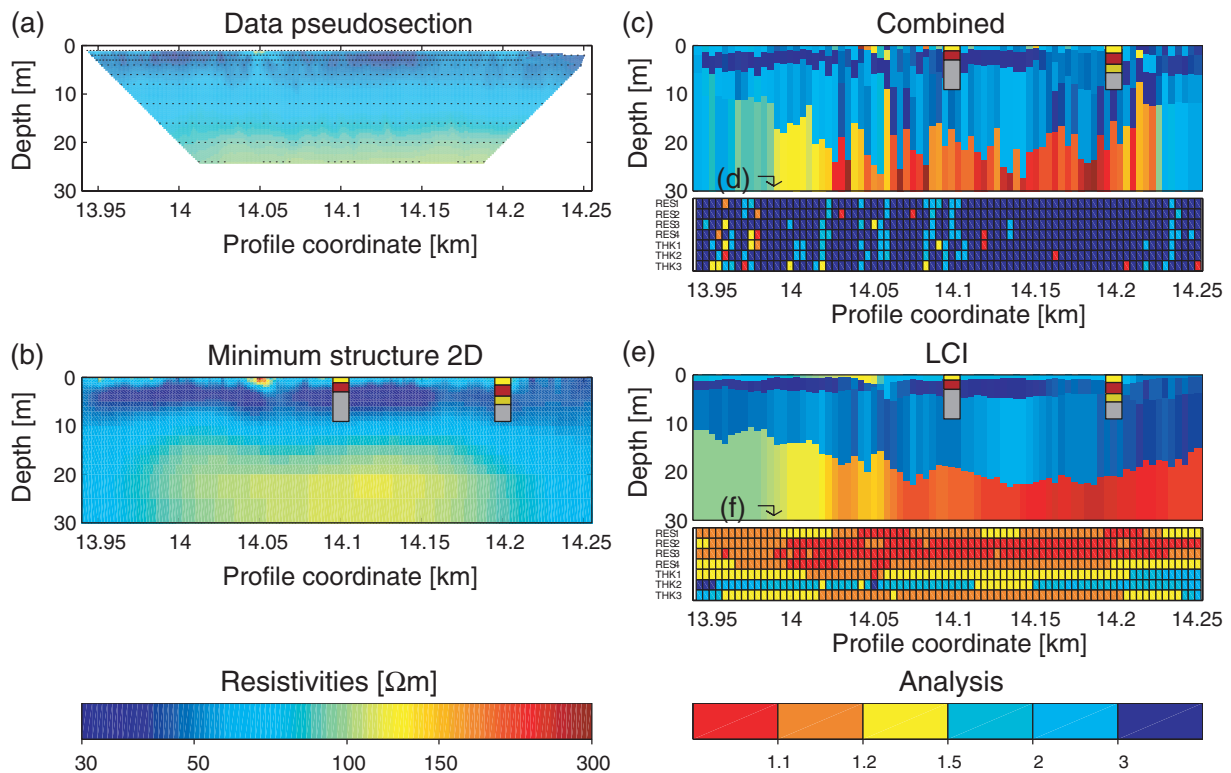


Figure 3 Field example: CVES. (a) A data pseudosection; (b) a minimum structure 2D inversion; (c) a combined section of 1D inversion with analyses in (d); (e) and (f) the LCI and parameter analyses. The colour coding of the analyses ranges from well-resolved (red) to poorly resolved (blue). Two drill-holes are located at 14.1 km and 14.2 km. The colours in the hole located at 14.2 km indicate, from the bottom: grey medium-fine clay (grey), silty sand (dark yellow), brown medium-fine clay (brown) and medium sands (yellow) at the top. In the drill-hole at 14.1 km the silty layer is missing, otherwise the results from the two drill-holes are the same.

of near-surface inhomogeneities along the profile. Down to a depth of approximately 10 m, there seems to be a relatively horizontal layer with resistivities about 40 Ωm above a more resistive basement. Formation boundaries cannot be recognized from the inverted section. Figure 3(c) shows a section of combined 1D inversions along the profile. Indications of formation boundaries are seen, but they have a geologically unrealistic appearance mainly because of equivalence problems. The analysis in Fig. 3(d) mainly shows poorly resolved parameters with only occasionally well-determined parameters. Figure 3(e), the laterally constrained inversion model section, shows a model using four layers with smooth transitions in resistivities and layer boundaries while still picking up the near-surface resistivity changes. We can now see a layered structure with a bowl-shape on the bottom layer along the profile, and we are able to differentiate between the two clay layers revealed by the drill-holes. The thicknesses of the top layer and

the brown clay layer are consistent with those found in the two drill-holes. The silty layer is not found, either because it is a very local structure, as indicated by the drill-holes, or because the resistivity of the layer is close to that of the clay layers. The analyses in Fig. 3(f) present mainly well-determined parameters along the profile. Only the thickness of the second layer is rather poorly determined, due to the low resistivity contrast with the third layer. All the model sections shown produce data that fit the observed data to an acceptable level.

PACES example, Jutland, Denmark

This is a typical example from a groundwater survey in Denmark. The purpose of these surveys is to determine absolute amounts of sand versus clay in the upper 15–20 m. Figure 4 shows the results comparing the laterally constrained inversion (Fig. 4b) and the minimum structure inversion obtained

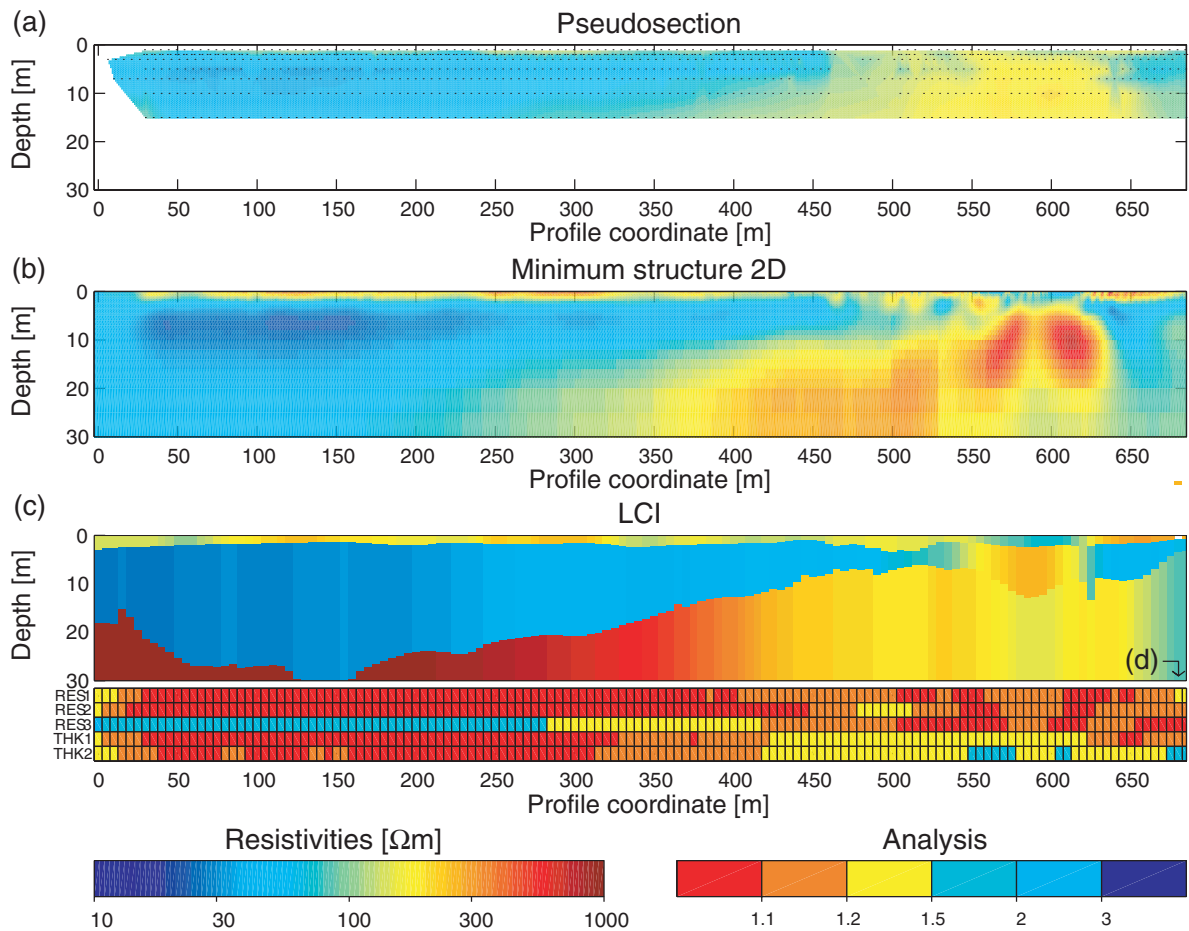


Figure 4 Field example: PACES. (a) The data pseudosection; (b) the LCI with analyses in (c); (d) the 2D minimum structure inversion obtained using DCINV2D. The sounding distance is 5 m and the total profile length is 700 m.

using the DCINV2D program (Fig. 4d). Data and the laterally constrained inversion model parameter analysis are shown in Fig. 4(a,c). The constraints between resistivities and depth interfaces used in the laterally constrained inversion form a factor of 1.14.

The data pseudosection in Fig. 4(a) shows relatively smooth transitions, but there is some evidence of 2D structures from around profile coordinate 500 m. The minimum structure 2D inversion (Fig. 4b) shows a smooth picture with a resistive layer on top of a more conductive layer. From around profile coordinate 300 m, a resistive body is seen beneath the top resistive layer, but the extent of the body is barely recognizable. The laterally constrained inversion section (Fig. 4c) shows a three-layer model with smooth lateral variations in all layers. The model gives a clear indication of a resistive top layer above a more conductive layer overlying a resistive bottom layer. The thickness of the conductive middle layer varies considerably along the profile from more than 20 m around coordinate 140 m to zero around coordinate 550–600 m. The analyses in Fig. 4(d) reveal well-determined parameters in most parts of the profile. The resistivity of the bottom layer is rather poorly determined at the beginning of the profile where the depth to the layer is considerable compared with the maximum layout of electrode configurations. The conductive middle layer is a clayey till, and it is extremely important for the hydraulic and chemical impact on a possible underlying aquifer.

If, in this case, we had had only the minimum structure 2D inversion section, we would have lost the detailed information about the thickness of the clay layer, and the hydrological interpretation of the survey would have been significantly different from the one obtained based on the piecewise 1D laterally constrained inversion interpretation.

DISCUSSION

Laterally constrained inversion or 2D minimum structure?

The near-surface geology in sedimentary areas most often consists of tills or glacial sands. The subsurface has an overall layering with minor resistivity variations within the individual layers. In this setting, it is rare that the 1D model assumption, in the sensitivity volume of the electrode configurations, is significantly violated. However, it is important to consider the dimensionality of the underlying model before applying a layered inversion scheme. Synthetic modelling with the PACES system set-up has shown that the laterally constrained inversion is capable of identifying 2D slope structures dipping up to 20% (Foged 2001). Above 20%, the 1D model is violated

too much, and the slope is smoothed. The resolution of such dipping structures depends on the configuration (Dahlin and Zhou 2004), but will always be limited under the 1D assumption.

2D or 3D variations introduced by near-surface resistivity variations are impossible to resolve with any 1D code, due to the spatial distribution of the sensitivities in the 4-pole configuration.

The use of the laterally constrained inversion algorithm for hydrogeophysical investigations

Since 1999, the piecewise 1D laterally constrained inversion algorithm has been used as the primary interpretation algorithm for more than 10 000 km of PACES data in hydrogeophysical surveys. The algorithm has proved its stability for interpretation of large data sets when the geological structures are quasi-layered and predominantly one-dimensional. When the subsurface has a layered appearance but with significant 2D structures, we suggest using the 2D development of the laterally constrained inversion algorithm (Auken and Christiansen 2004). Recently, CVES data collected in Denmark and Sweden have been experimentally interpreted using both the laterally constrained inversion algorithm and the smooth 2D minimum structure inversion produced by the RES2DINV program or the DCINV2D program (Wisén, Auken and Dahlin 2002). This combination of inversion strategies has proved to be powerful as a basis for the geological/hydrogeological interpretation. The geological interpretation is primarily based on models produced by piecewise 1D laterally constrained inversion, and the 2D minimum structure inversion is used to reveal areas where lateral resistivity variations in the subsurface unacceptably violate the 1D model assumption in the piecewise 1D laterally constrained inversion.

CONCLUSION

The piecewise 1D laterally constrained inversion method provides a robust and quick method to obtain reliable inversion results in semi-layered environments from continuous resistivity data. The layered model description makes identification of formation boundaries easy, compared with standard minimum structure 2D algorithms, which produce a smeared picture of the geological model. The inclusion of lateral constraints improves the resolution of poorly resolved parameters. This is clearly demonstrated by model sections comparing 1D sections with and without lateral constraints. Prior knowledge

can be added at any point along the model profile, and the output is supported by a full sensitivity analysis of the model parameters entering the inversion scheme. Thus, it is possible for the interpreter to ascertain the inversion result.

ACKNOWLEDGEMENTS

We thank Professor Douglas Oldenburg at the University of British Columbia for letting us use the 2D resistivity code for forward calculations and inversions. Professor Torleif Dahlin kindly provided the CVES field data. Professor Niels B. Christensen helped us clarify the paper and has contributed with numerous helpful comments.

REFERENCES

- Albouy Y., Andrieux P., Rakotondrasoa G., Ritz M., Desclotres M., Join J.-L. and Rasolomanana E. 2001. Mapping coastal aquifers by joint inversion of DC and TEM soundings: Three case histories. *Ground Water* **39**, 87–97.
- Auken E. and Christiansen A.V. 2004. Layered and laterally constrained 2D inversion of resistivity data. *Geophysics* **69**, 752–761.
- Auken E., Foged N. and Sørensen K.I. 2002. Model recognition by 1-D laterally constrained inversion of resistivity data. *Proceedings of the New Technologies and Research Trends Session*, 8th EEGS-ES meeting, Aveiro, Portugal.
- Bernstone C. and Dahlin T. 1999. Assessment of two automated DC resistivity data acquisition systems for landfill location surveys: Two case studies. *Journal of Environmental and Engineering Geophysics* **4**, 113–121.
- Christensen N.B. 1990. Optimized fast Hankel transform filters. *Geophysical Prospecting* **38**, 545–568.
- Christiansen A.V. and Auken E. 2003. Optimizing the 2D laterally constrained inversion (2D-LCI) using a quasi-Newton method and 1D derivatives. *Proceedings of the New Technologies and Research Trends Session*, 9th EEGS-ES meeting, Prague, Czech Republic.
- Dahlin T. 1996. 2D resistivity surveying for environmental and engineering applications. *First Break* **14**, 275–283.
- Dahlin T. 2001. The development of DC resistivity imaging techniques. *Computers and Geosciences* **27**, 1019–1029.
- Dahlin T. and Zhou B. 2004. A numerical comparison of 2D resistivity imaging with 10 electrode arrays. *Geophysical Prospecting* **52**, 379–398.
- Dey A. and Morrison H.F. 1979. Resistivity modelling for arbitrarily shaped 2-dimensional structures. *Geophysical Prospecting* **27**, 106–136.
- Dodds A.R. and Ivic D. 1990. Integrated geophysical methods used for groundwater studies in the Murray Basin, South Australia. In: *Geotechnical and Environmental Geophysics* (ed. S.H. Ward), Vol. 1, pp. 303–310. Investigations in Geophysics 5. Society of Exploration Geophysicists.
- Fitterman D.V. 1987. Examples of transient sounding for groundwater exploration in sedimentary aquifers. *Ground Water* **25**, 684–693.
- Fitterman D.V., Meekes J.A.C. and Ritsema I.L. 1988. Equivalence behaviour of three electrical sounding methods as applied to hydrogeological problems. 50th EAEG meeting, The Hague, The Netherlands, Expanded Abstracts.
- Foged N. 2001. *Laterally constrained inversion of 2-D stochastic earth structures*. MSc thesis, University of Aarhus, Denmark.
- Gyulai Á. and Ormos T. 1999. A new procedure for the interpretation of VES data: 1.5-D simultaneous inversion method. *Journal of Applied Geophysics* **64**, 1–17.
- Inman J.R. Jr, Ryu J. and Ward S.H. 1975. Resistivity inversion. *Geophysics* **38**, 1088–1108.
- Johansen H.K. 1977. A man/computer interpretation system for resistivity soundings over a horizontally stratified earth. *Geophysical Prospecting* **25**, 667–691.
- Johansen H.K. and Sørensen K.I. 1979. Fast Hankel transforms. *Geophysical Prospecting* **27**, 876–901.
- Loke M.H. and Barker R.D. 1996. Rapid least-squares inversion of apparent-resistivity pseudosections by a quasi-Newton method. *Geophysical Prospecting* **44**, 131–152.
- Loke M.H., Acworth I. and Dahlin T. 2003. A comparison of smooth and blocky inversion methods in 2-D electrical imaging surveys. *Exploration Geophysics* **34**, 182–187.
- McGillivray P.R. 1992. *Forward modeling and inversion of DC resistivity and MMR data*. PhD thesis, The University of British Columbia, Vancouver, Canada.
- Menke W. 1989. *Geophysical Data Analysis – Discrete Inverse Theory*, revised edn. International Geophysics Series. Academic Press, Inc.
- Oldenburg D.W. and Ellis R.G. 1991. Inversion of geophysical data using an approximate inverse mapping. *Geophysical Journal International* **105**, 325–353.
- Oldenburg D.W. and Li Y. 1994. Inversion of induced polarization data. *Geophysics* **59**, 1327–1341.
- Panissod C., Lajarthe M. and Tabbagh A. 1997. Potential focusing: a new multi-electrode array concept, simulating study, and field tests in archaeological prospecting. *Geophysics* **38**, 1–23.
- Robineau B., Ritz M., Courteaud M. and Desclotres M. 1997. Electromagnetic investigations of aquifers in the Grand Brulé coastal area of Piton de la Fournaise volcano, Reunion Island. *Ground Water* **35**, 585–592.
- Sandberg S.K. and Hall D.W. 1990. Geophysical investigation of an unconsolidated coastal plain aquifer system and the underlying bedrock geology in Central New Jersey. In: *Geotechnical and Environmental Geophysics* (eds S.H. Ward), Vol. 1, pp. 311–320. Investigations in Geophysics 5. Society of Exploration Geophysicists.
- Santos F.A.M. 2004. 1-D laterally constrained inversion of EM34 profiling data. *Journal of Applied Geophysics* **56**, 123–134.
- Smith J.T. and Booker J.R. 1991. Rapid inversion of two and three-dimensional magnetotelluric data. *Journal of Geophysical Research* **96**, 3905–3922.

- Sørensen K.I. 1996. Pulled array continuous electrical profiling. *First Break* 14, 85–90.
- Sørensen K.I., Auken E., Christensen N.B. and Pellerin L. 2005. *An Integrated Approach for Hydrogeophysical Investigations: New Technologies and a Case History*. Near Surface Geophysics Vol. II: Applications and Case Histories. Society of Exploration Geophysicists, in press.
- Tarantola A. and Valette B. 1982. Generalized nonlinear inverse problems solved using a least squares criterion. *Reviews of Geophysics and Space Physics* 20, 219–232.
- Taylor K., Widmer M. and Chesley M. 1992. Use of transient electromagnetics to define local hydrogeology in an arid alluvial environment. *Geophysics* 57, 343–352.
- Telford W.M., Geldart L.P. and Sheriff R.E. 1990. *Applied Geophysics*, 2nd edn. Cambridge University Press.
- Van Overmeeren R.A. and Ritsema I.L. 1988. Continuous vertical electrical sounding. *First Break* 6, 313–324.
- Ward S.H. and Hohmann G.W. 1988. Electromagnetic theory for geophysical applications. In: *Electromagnetic Methods in Applied Geophysics* (ed. M.N. Nabighian), Vol. 1(4), pp. 131–311. Society of Exploration Geophysicists.
- Wisén R., Auken E. and Dahlin T. 2002. Comparison of 1D laterally constrained inversion and 2.5D inversion of CVES resistivity data with drilling data as a *priori* information. *Proceedings of the New Technologies and Research Trends Session*, 8th EEGS-ES meeting, Aveiro, Portugal.